First-principles investigation of electronic, vibrational, elastic, and structural properties of ThN and UN up to 100 GPa

P. Modak and Ashok K. Verma*

High Pressure and Synchrotron Radiation Physics Division, Bhabha Atomic Research Centre, Trombay, Mumbai 400 085, India

(Received 27 January 2011; revised manuscript received 4 May 2011; published 6 July 2011)

We have investigated the electronic properties, phonon dispersion relations, elastic constants, structural phase transitions, and pressure-volume equations-of-state of thorium (Th) and uranium (U) mononitrides (ThN and UN) under pressure (0−100 GPa) using pseudopotential density functional theoretical methods. The generalized gradient approximation (GGA) is found to describe the ground-state and high-pressure experimental data much better than the local density approximation (LDA) for both compounds. ThN shows acoustic mode phonon softening along the Γ−X direction of the Brillouin zone in the NaCl phase under pressure, followed by a transition to a CsCl structure at 72.5 GPa. Detailed electronic structure analysis revealed an electronic topological transition under pressure that could be responsible for acoustic mode phonon softening and structural phase transition. Unlike ThN, UN shows a structural phase transition from an NaCl to R-3m structure at a much smaller pressure (18 GPa), and the calculated C_{44} shear elastic constant decreases with pressure and becomes negative at 15 GPa. A Peierls-like distortion, due to *f* states, is found responsible for elastic instability and structural phase transition. Our results are in reasonably good agreement with available experimental data. We have also tested the effect of on-site Coulomb interactions on a few ground-state properties and on the phase-transition behavior of UN.

DOI: 10.1103/PhysRevB.84.024108 PACS number(s): 71.15.Mb, 64.70.K−, 63.20.dk, 62.20.de

I. INTRODUCTION

In recent times actinide mononitrides (AcN) have been studied extensively because of their possible use as advanced fuels in the fourth generation nuclear reactors.[1] In comparison to present oxide fuels, the nitride fuels have superior thermophysical properties (i.e., high thermal conductivity and high melting temperature), higher burn-up, easy re-processing, and higher metal (actinides) density.[2] Also, these compounds are important target materials for the transmutation of minor actinides ($_{93}$ Np and beyond).[3] Further interest in the actinides and their compounds is due to the 5*f* electrons whose behavior is intermediate to strongly localized 4*f* electrons of lanthanides and itinerant *d* electrons of transition metals. The competition between localization and itinerancy of 5*f* electrons produces spectacular electronic and magnetic properties. The 5*f* electrons, which behave like itinerant electrons, participate actively in metallic bonding in light actinides ($_{90}$Th − $_{93}$Np), whereas in heavy actinides ($_{95}$Am and beyond), the degree of localization of the 5*f* electrons increases as one moves toward higher atomic number elements,[4] leading to the reduction of their contribution to the chemical bonding. The rapid decrease of atomic volumes of light actinides with an increase in atomic number correlates well the more 5*f* electrons participation in chemical bonding.[5]

Although many theoretical[2–10] and experimental[11–14] studies have been carried out in the past on actinide nitrides, especially to understand the behavior of 5*f* electrons and their effect on the physical, chemical, thermal, and magnetic properties, very few studies have investigated the high-pressure behavior of 5*f* electrons and their effects on physical and chemical properties and on the possible structural phase transitions.[15,16] To explore the role of 5*f* electrons on various properties, we have carried out detailed investigations of chemical bonding, pressure-volume (*PV*) relations, elastic constants, and vibrational properties of the thorium (Th) and uranium (U) mononitrides (ThN and UN) using first-principles pseudopotential methods. It is worth mentioning that both ThN and UN crystallize in rock salt (i.e., NaCl) structure at ambient conditions,[15,16] although the constituent Ac metals have different 5*f* state occupancies. Because of high-lying 5*f* states in Th, it is expected that 5*f* electrons will contribute minimally to chemical bonding in ThN. However, for UN, chemical bonding is expected to be dominated by 5*f* electrons, similar to uranium metal. Therefore, the comparative study of these systems is expected to provide useful insight on the possible role of 5*f* electrons on ground-state and high-pressure properties.

In this work, we have shown that the local-density approximation (LDA)[17] is inadequate in describing ground-state and high-pressure properties of ThN and UN; however, the generalized-gradient approximation (GGA)[18] works very well for ThN and also gives reasonable results for UN. We have also calculated phonon dispersion relations and elastic constants for both compounds with the GGA exchange correlations over the 0−100-GPa region. In ThN, the GGA (LDA) calculation shows a NaCl to CsCl structural transition at 72.5 (62.5) GPa. Acoustic-mode phonon softening along the Γ−X direction of the Brillouin zone (BZ) was also obtained near this transition. A pressure-induced electronic topological transition at the X point is found to be responsible for phonon softening and a structural phase transition. However, UN undergoes a structural phase transition from NaCl to a rhombohedral structure (space group R-3m) and the GGA (LDA) calculated transition pressure is 18 (4.7) GPa. Also, both compounds are shown to be mechanically unstable in R-3m phase at zero pressure, but this phase of UN becomes mechanically stable near the transition pressure. We have also shown that the parent NaCl structure becomes elastically unstable near 15 GPa. Presence of the main peak of the U *f* states at the Fermi level and its enhanced hybridization with U *d* and N

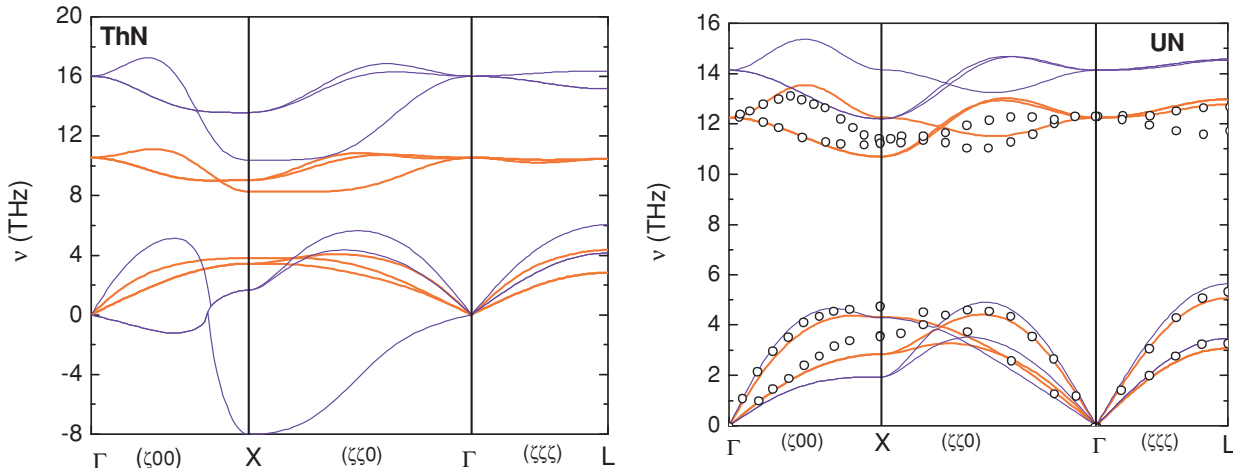

FIG. 1. (Color online) The GGA phonon dispersion curves for ThN and UN at zero pressure (red thick lines) and at transition pressure (thin blue lines). Experimental data (open circles) are taken from Ref. 34.

p states under pressure is found to be responsible for elastic instability and the high-pressure structural phase transition.

II. METHODOLOGY

We have calculated 0 K total energies of ThN and UN in three structures—viz., NaCl, CsCl, and R-3m—as a function of volume to determine the ground-state lattice constants, bulk moduli, structural phase transitions, and PV relations. The ground-state lattice constants and bulk moduli are estimated by fitting the energy-volume data to third-order Birch–Murnaghan equation-of-state relations.[19] To study the transition path between these structures, we have calculated enthalpy as a function of c/a ratios at a few pressures because these three structures can be cast into a rhombohedral unit cell (space group R-3m). In both rhombohedral and cubic systems, the crystal cells are described by three vectors of equal length. The only difference between these crystal systems is that the cell vectors are orthogonal in a cubic system, whereas they are nonorthogonal in a rhombohedral system. Rhombohedral cells having angles 60°, 90°, and 109.47° represent primitive cells of face-centered cubic (fcc), simple cubic, and body-centered cubic (bcc) systems, respectively. A primitive rhombohedral unit cell can easily be converted into a triple-hexagonal cell with three lattice points at (0, 0, 0), (2/3, 1/3, 1/3), and (1/3, 2/3, 2/3). The lattice constants (a_h and c_h) of the hexagonal cell can be obtained from the rhombohedral lattice parameters (a_r and α_r) using the following relations:

$$\begin{aligned} a_h &= 2a_r \cos(\pi - \alpha_r)/2 \\ c_h &= 3\sqrt{\left(a_r^2 - a_h^2/3\right)} \end{aligned} \tag{1}$$

Therefore, just by changing c/a ratios in a hexagonal setting, we can obtain NaCl, CsCl, and R-3m structures. The vibrational stability of the NaCl structure at zero and high pressure was examined by calculating the phonon dispersion relations using small displacement supercell methods,[20] and elastic stability was examined by calculating the elastic constants.[21]

All the calculations in this work were carried out using a method based on the plane wave pseudopotential density functional theory, as implemented in the Vienna *Ab-initio* Simulation Package (VASP).[22–25] Projector-augmented wave (PAW) pseudopotentials were used with a 1000-eV plane wave energy cutoff, and both the local density approximation (LDA)[17] and the generalized gradient approximation (GGA)[18] were employed. We have also tested the effect of on-site Coulomb interactions for U f states by carrying out GGA + U[26] calculations in NaCl and R-3m phases of UN. Here, the U (5.2 eV) and J (0.5 eV) parameters were taken from Ref. 27 and were estimated using the self-consistent GW method. The Th, U, and N pseudopotentials were generated by taking $6s^2, 6p^6, 6d^2, 7s^2$; $5f^3, 6s^2, 6p^6, 6d^1, 7s^2$; and $2s^2, 2p^3$ as the valence state configurations, respectively. For Brillouin zone integrations, a uniform Monkhorst–Pack mesh[28] with a total of 5000 **k** points in the full Brillouin zone was used.

The phonon dispersion relations were calculated using the small displacement force method, in which the force constant matrix (given as the second derivative of energy with respect to displacements of atoms from their equilibrium positions) was constructed by calculating the forces on atoms of a periodically repeated supercell that arise due to the displacement of a few selected atoms from their equilibrium positions. The dynamical matrix can be easily constructed from the force constant matrix, which can be diagonalized to get the phonon frequencies (see for detail Ref. 20). Here, we have taken a $3 \times 3 \times 3$ supercell (27 Ac + 27 N), and the PHON code[29] was used to determine the displacement pattern, as well as to solve the dynamical matrix. Two atoms were displaced one by one, according to the displacement patterns generated by PHON code, by an amount of 0.04 Å, and then the self-consistent forces on the atoms were determined. In the force calculations, we have taken a $4 \times 4 \times 4$ Monkhorst–Pack mesh[28] for BZ integrations.

According to Hook's law, the elastic energy of a solid can be written as a quadratic function of the strain components; hence, the elastic constants can be derived from the second-order

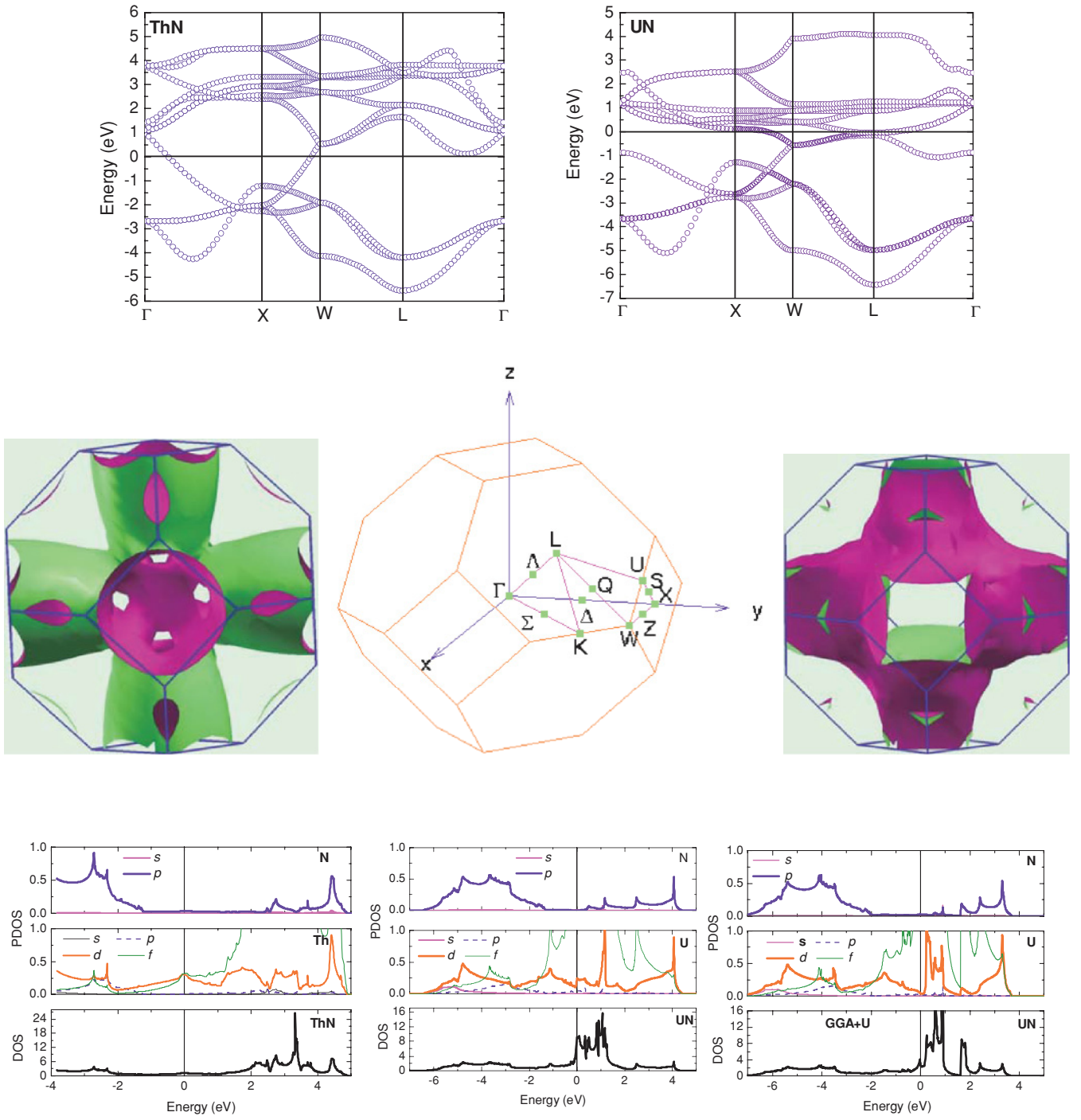

FIG. 2. (Color online) The GGA electronic band structures (top panel), Fermi surfaces and fcc BZ (middle panel), and total and partial electronic density of state (DOS) functions (bottom panel) of ThN and UN in the NaCl structure at zero pressure. Right plot of the bottom panel shows the GGA + U DOS functions of UN at zero pressure. The electronic band structures are shown only in the high-symmetry directions of the Brillouin zone. The unit of DOS is states/eV-f.u.

derivatives of the energy–strain relations. A cubic crystal has three independent elastic constants—C_{11}, C_{12}, and C_{44}—and so a set of three equations is needed to determine all three elastic constants. For this, we employed following three sets of calculations: the first set determines bulk modulus $[B = (C_{11} + 2C_{12})/3]$ through the energy-volume relationship; the second set determines tetragonal shear constant $[C' = (C_{11} - C_{12})]$ through the energy–tetragonal strain relationship; and the third set determines $[(C_{11} + 2C_{12} + 4C_{44})/3]$ through the energy–rhombohedral strain relationship. In the third set of calculations, total energy is calculated as a function of the length of the great diagonal of the cubic cell. For each set, we

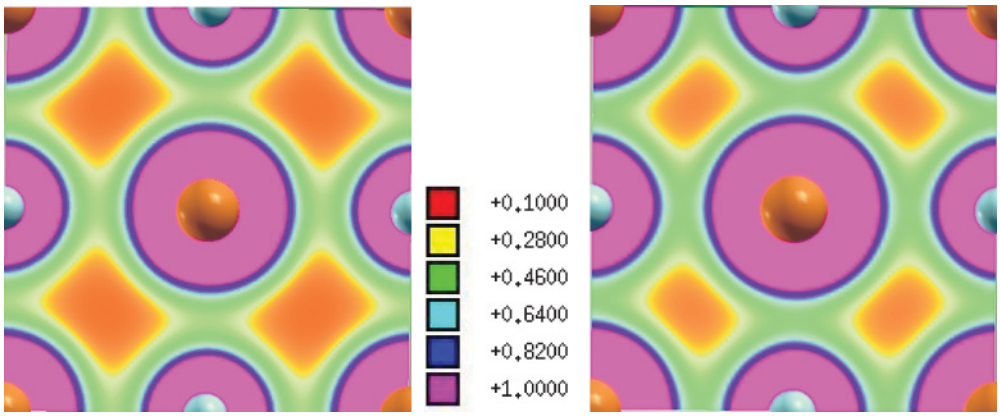

FIG. 3. (Color online) The GGA electron charge density distributions in (100) plane for ThN and UN at zero pressure. The unit of charge density is the number of electrons per Å^3. The spheres at the edge centers are Ac atoms (brown), and spheres at the center edges are N atoms (blue).

have applied five strains. In these calculations, a denser **k** point mesh (10 000 points) is used for BZ integrations.

III. RESULTS AND DISCUSSION

A. Ground-state properties

Although ThN and UN crystallize in rock salt (NaCl) structure at ambient conditions, their lattice constants differ considerably: the UN lattice constant is ∼5% smaller than ThN. The smaller lattice constant indicates the stronger chemical bonding in UN, which is further supported by its larger bulk modulus value (see Table I). The lattice constants, bulk moduli and elastic constants of both compounds calculated at ambient pressure are compared in Table I with the available theoretical and experimental results.[10,15,16] LDA/GGA underestimates the lattice constants by 1.28/−0.19% and 2.21/0.63% for ThN and UN, respectively, compared with that of experimental data. The LDA bulk modulus differs considerably from the experimental values: the LDA overestimates the bulk moduli by 21% and 31% for ThN and UN, respectively. However the GGA bulk moduli differ by 3% and 11% for ThN and UN, respectively. The good agreements of the GGA results with the experimental data indicate the importance of nonhomogeneous electron density contributions in describing the ground-state properties of these compounds. Although the GGA + U calculations for UN improves the ambient pressure lattice constant slightly (see Table I), it fails to improve the bulk modulus, consistent with the earlier self-interaction–corrected local spin-density calculations.[30] Therefore, we decided to carry out rest of the calculations with the GGA exchange correlations. The spin-orbit coupling interactions were neglected because they are known to be small in these compounds.[10] Although the calculated C_{11} elastic constant for UN matches very well with that obtained from the ultrasonic wave velocity measurements,[31] the same is not true for other elastic constants: C_{12} is overestimated (39.2%), and C_{44} is underestimated (60.7%). The C_{11} elastic constant is known to include major contributions only from the nearest neighbor forces, whereas other elastic constants also have large contributions from the long-range forces.[31,32] Thus, the comparison of theoretical and experimental elastic constants indicates that although the GGA correctly describes the nearest neighbor U−N interactions, it fails to estimate correctly the long-range interactions, particularly the U−U interactions, which are known to be large in this compound.[32] For nearly ideal ionic solids such as NaCl, $C_{12} \cong C_{44}$, in that interionic forces are primarily central and the nonequality of these elastic

TABLE I. Calculated ambient pressure lattice constants (a), bulk moduli (B_0), pressure derivatives of bulk modulus (B_0'), and elastic constants (C_{11}, C_{12}, and C_{44}) of ThN and UN, together with previous theoretical and experimental results. Elastic constants are calculated for GGA exchange correlations. The pressure derivatives of elastic constants are shown inside the parentheses.

		a (Å)	B_0 (GPa)	B_0'	Elastic constants (GPa)
ThN	LDA	5.101	211.5	3.52	
	GGA	5.177	180.8	4.49	C_{11}: 333.0 (5.46)
	Expt.[15]	5.167	175.0	4.00	C_{12}: 103.1 (1.31)
	Others[10]	5.181	178.0		C_{44}: 74.0 (−0.65)
UN	LDA	4.781	266.3	3.63	C_{11}: 428.0 (6.50) Expt.[31]: 423.9 (9.97)
	GGA	4.858	225.0	4.00	C_{12}: 136.6 (2.76)
	GGA + U	4.899	233.2	6.28	Expt.[31]: 98.1 (3.81)
	Expt.[16]	4.889	203.0	6.30	C_{44}: 29.7 (−2.43)
	Others[10]	4.858	227.0		Expt.[31]: 75.7 (−0.74)

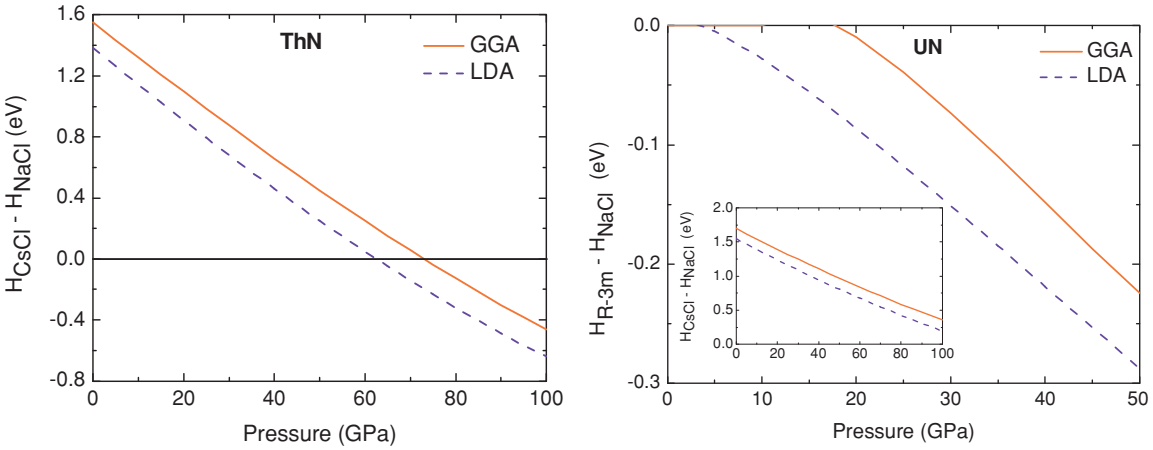

FIG. 4. (Color online) Pressure variation of GGA and LDA enthalpies (eV/formula unit (f.u.)) of ThN in the CsCl phase and UN in the R-3m phase with respect to their ambient NaCl phase. The inset shows the enthalpy variation of the CsCl phase.

constants is generally related with the noncentral forces that are present in the covalent or metallic bonded solids. Hence, by comparing calculated elastic constants, we can say that ThN ($C_{12}/C_{44} = 1.39$) is more ionic than UN ($C_{12}/C_{44} = 4.60$). It is to be noted that both compounds satisfy the elastic stability criterion:[21,33] $C_{11} + 2C_{12} > 0$; $C_{44} > 0$, and $C_{11} - C_{12} > 0$.

Figure 1 shows the phonon dispersion relations for ThN and UN at ground-state lattice constants as given in Table I. Both compounds show nearly flat dispersion curves for optical-mode phonons, which are expected because of large mass differences between constituent atoms ($M_U/M_N \cong 17.00$ and $M_{Th}/M_N \cong 16.57$) and large separations between neighboring lighter atoms ($d_{Th-N} = 2.59$ Å, $d_{N-N} = 3.66$ Å for ThN; d_{U-N} =\break 2.43 Å, $d_{N-N} = 3.43$ Å for UN). The calculated phonon dispersions for UN show excellent agreement with the inelastic neutron scattering data.[34] The overall higher optical phonon frequencies of UN compared with ThN indicate the stronger U−N bonds that result from the participation of 5*f* electrons in the chemical bonding.

Figure 2 (top panel) displays the electronic band structures of ThN and UN at ambient pressure. Both compounds show metallic behavior, having partially filled bands at the Fermi level (E_F). For ThN, the partially filled bands close to the Fermi level have nearly equal *d* and *f* characters, which originate from the hybridization of Th *d* and *f* states. For UN, the partially filled states close to the Fermi level have much higher *f* characters. The flat band is essentially the actinide *f* band, which lies 2 eV above the Fermi level in ThN, and it is just above the Fermi level in UN, leading to strong hybridization among U *d* and *f* states and N *p* states in the vicinity of the Fermi level. In both compounds, only one hybridized band cuts the Fermi level along different directions in the BZ, giving rise to multiply connected Fermi surfaces (see Fig. 2, middle panel). In ThN, as this band cuts E_F along the Γ−X direction, the cylindrical electron surface around X has a closed end toward Γ, whereas in UN, the corresponding surface has both ends open. Also, the cross section of this surface on the square face of BZ has different shapes in ThN and UN.

Figure 2 (lower panel) shows total, atom, and orbital projected electronic density of state (DOS) functions for both compounds. The bonding and antibonding N *p* states are well separated: in ThN, separation is ∼3.5 eV, whereas it is 1.7 eV in

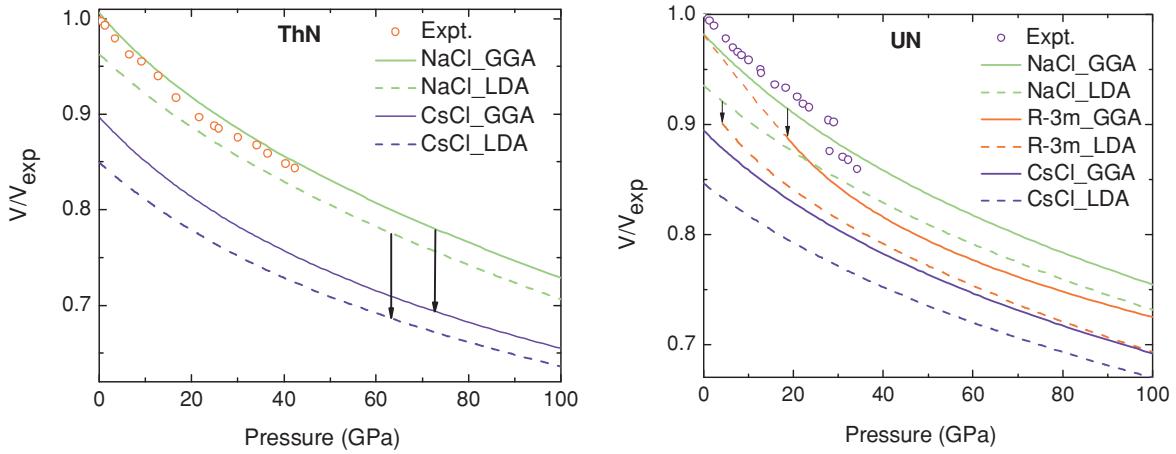

FIG. 5. (Color online) The GGA and LDA *PV* equation-of-state relations for ThN and UN in different phases. Initial dashed portion of the R-3m phase of UN shows the extrapolated data, in that this phase is mechanically unstable in this region. Experimental data are taken from Refs. 15 and 16, and arrows indicate the respective transition pressures.

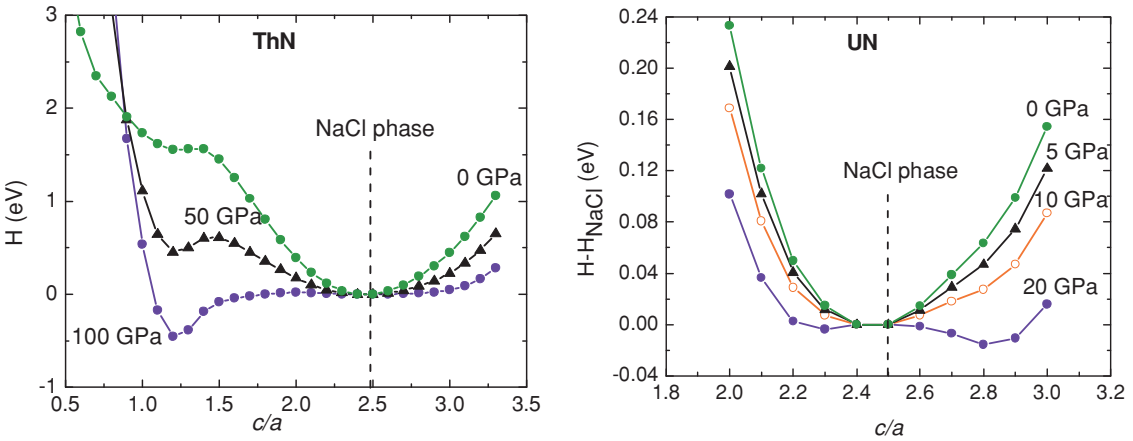

FIG. 6. (Color online) The GGA enthalpy barriers (eV f.u.$^{-1}$) at different pressures for ThN and UN.

UN. ThN total DOS at E_F (1.15 states/eV-f.u.) is much smaller (∼8 times) than that of UN (9.21 states/eV-f.u.), indicating that ThN has poorer electrical and thermal conductivities than UN. With GGA + U calculations, the DOS at E_F for UN reduces to 2.96 states/eV-f.u. but still it is higher than that of ThN. The DOS at E_F reduces mainly because of the reduction of the f partial DOS peak and d partial DOS at E_F. Also, GGA + U opens a gap between $f_{5/2}$ and $f_{7/2}$ states above E_F. ThN metallic behavior comes from the partially filled Th d and f states. Although the Th f states are mostly unoccupied, its contribution to total DOS at E_F comes from the hybridization effects. UN metallicity is due to the U d and f states. Therefore, DOS analysis shows that although both mononitrides crystallize in the NaCl structure at zero pressure, their bonding characteristics differ considerably, which is also reflected in the charge density plots (Fig. 3). Most of the charge density is concentrated around atomic sites in both compounds, but noticeable differences exist between them: The interstitial regions have a smaller charge density in ThN than UN, and ThN has a smaller charge density in the regions between the nearest neighbors. Thus, ThN is a better ionic solid than UN.

B. High-pressure properties

From crystal structure relaxation calculations, we find that the R-3m structure relaxes to the NaCl structure for both compounds at zero pressure. Under pressure, ThN shows a phase transition from the NaCl to the CsCl structure at 72.5 GPa, but the R-3m structure remains unstable up to 100 GPa. However, for UN, the R-3m structure becomes stable under pressure, and near 18 GPa, it becomes both energetically and mechanically stable (Fig. 4). However, the CsCl structure remains energetically unstable for UN up to 100 GPa. At 20 GPa, the computed lattice parameters for the R-3m phase are 3.4935 Å, and the rhombohedral angle is 53.8°. These results are in good agreement with the earlier high-pressure x-ray diffraction measurements,[15,16] wherein no structural phase transition was observed up to 47 GPa in ThN, and a structural transition (NaCl to R-3m) was observed in UN near 29 GPa. The transition pressure mismatch in UN is probably due to the inability of density function theory to treat narrow f bands properly. In fact, the GGA + U calculations predict better agreement in transition pressure (26 GPa) with

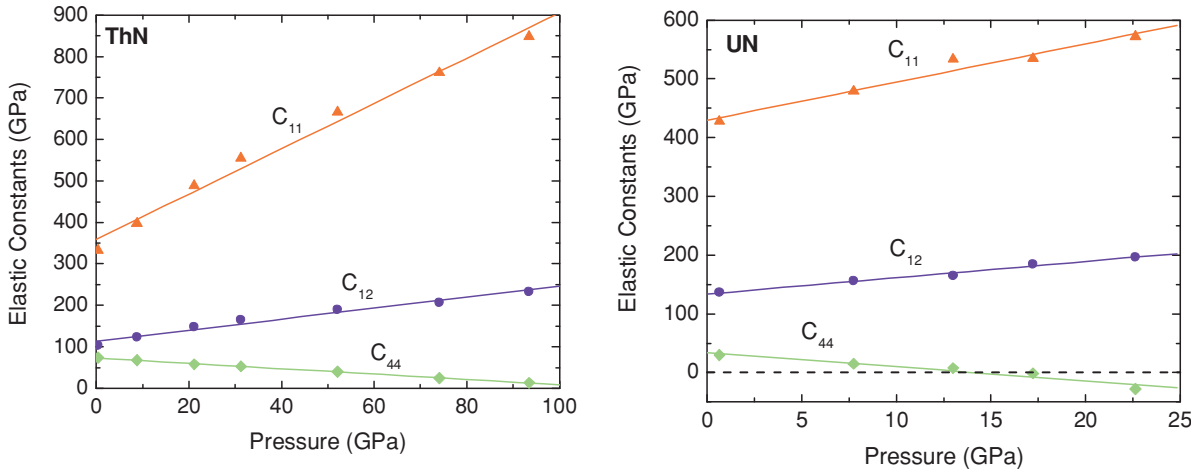

FIG. 7. (Color online) Pressure variation of the elastic constants of UN and ThN in the NaCl phase.

that of the experiment. However, it is to be noted that, in these calculations, we have used the same Hubbard U and exchange J parameters for NaCl and R-3m structures and also kept them fixed under pressure. But these parameters are expected to change not only with pressure, but also with the crystal structure. It is worth mentioning that the LDA transition pressures are 4.7 and 62.5 GPa for UN and ThN, respectively. Therefore, in both cases, the LDA underestimates transition pressure, but for UN, this underestimation is very large (84%). The calculated PV equation-of-states relations together with experimental results are shown in Fig. 5. A large volume reduction (11.0%) is seen during NaCl to CsCl phase

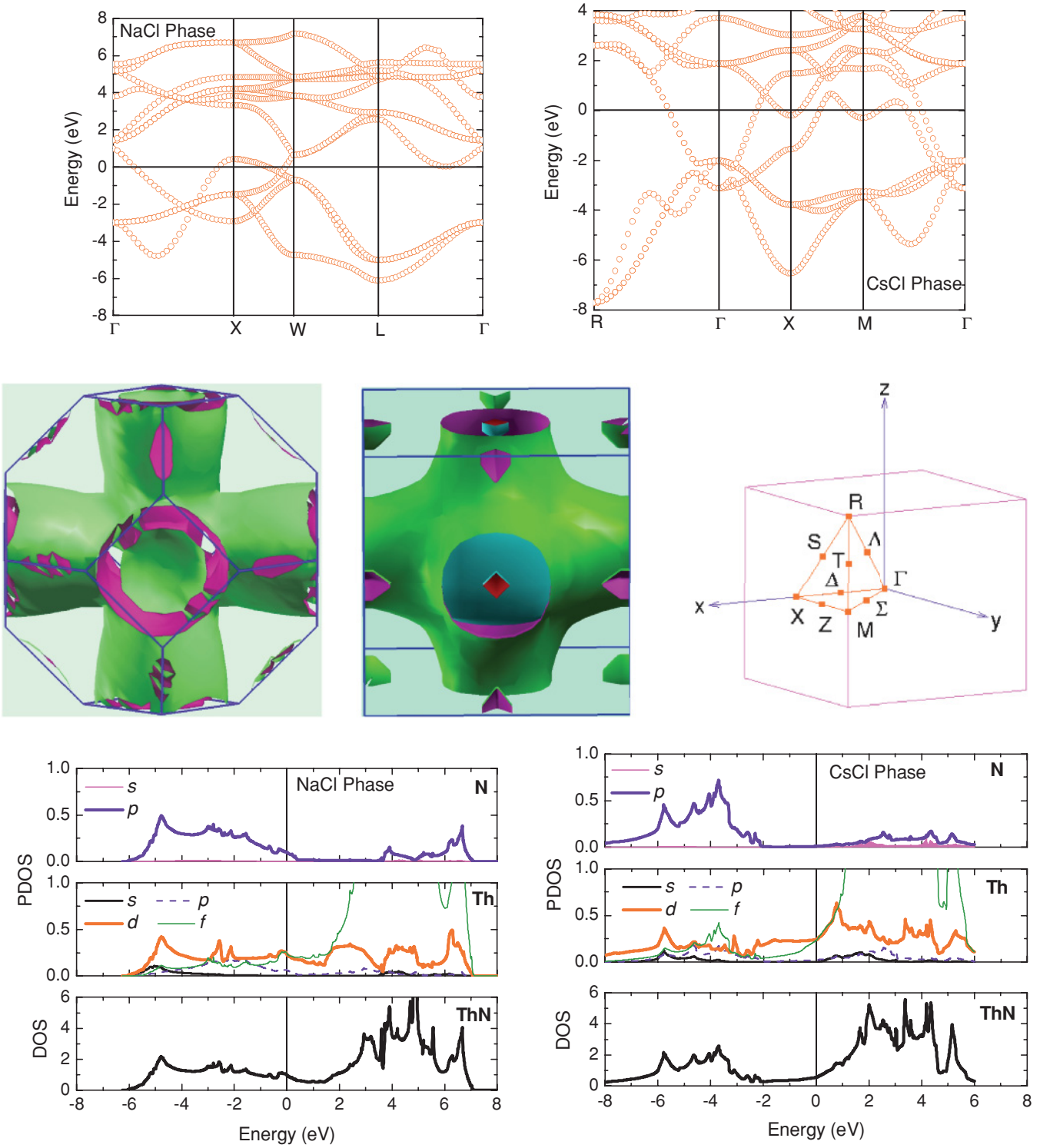

FIG. 8. (Color online) The GGA electronic band structure (top panel), Fermi surfaces along with simple cubic BZ (middle panel), and total and partial density of state (DOS) functions (bottom panel) of ThN at a volume of 26.99 Å^3 f.u.$^{-1}$. The density of state (DOS) functions are given in units of states/eV-f.u.

transitions in ThN, whereas a small volume change (2.5%) is found during NaCl to R-3m phase transitions in UN, which is consistent with the experimentally observed value of 3.2%.[16]

To trace the transition path between NaCl and CsCl structures, we carried out enthalpy calculations as a function of c/a ratios for the R-3m structure at a few pressures (Fig. 6). At zero pressure, the enthalpy minimum occurs at a c/a ratio of 2.449 for both compounds. This c/a value represents the NaCl structure, which is consistent with the fact that the NaCl structure is the ground-state structure of these compounds. In ThN, the CsCl structure, $c/a = 1.225$, gives a local minimum above 1.55 eV per formula unit (f.u.) at zero pressure. But the barrier height decreases with pressure, and finally the local minimum becomes the global minimum. Calculated phonon dispersions in the NaCl structure (see Fig. 1) near the transition pressure also show acoustic-mode phonon softening along $\Gamma-X$ direction of the BZ. The pressure variation of elastic constants is presented in Fig. 7. In ThN, although the C_{44} elastic constant decreases with pressure, it remains positive over the entire pressure region of our study. In UN, the local enthalpy minimum corresponding to the CsCl structure always lies above the global minimum, and the enthalpy barrier relative to the NaCl structure is 0.45 eV f.u.$^{-1}$ at 100 GPa (see Fig. 4, inset). However, a new local minimum around $c/a = 2.80$ develops under pressure progressively, which becomes the global minimum at 18 GPa (see Fig. 6). It is interesting to note that, at this pressure, the NaCl structure sits at a local maximum. The phonon calculations for the NaCl structure at high pressure (see Fig. 1) show anomalous high-pressure behavior for transverse acoustic modes along the $\Gamma-X$ direction of the BZ, which indicates the development of some sort of vibrational instability in the system under pressure for the NaCl structure. In fact, our calculated C_{44} elastic constant becomes negative near 15 GPa (see Fig. 7), indicating the loss of elastic stability for the NaCl structure. Thus, the uranium mononitrides in the NaCl structure become elastically unstable near the transition pressure. This is very similar to what was earlier predicted for vanadium metal, although in vanadium metal, the R-3m phase stabilizes before the C_{44} elastic constant becomes negative in the bcc phase.[35–38]

To understand the electronic origin of the structural phase transitions, we carried out an analysis of electronic structures of both compounds. Figure 8 (top panel) shows the electronic band structures, Fermi surfaces, and DOS functions of ThN in the NaCl structure at a volume near the phase transition. It is clear that the N p band maximum at point X, which was at 1 eV below E_F at zero pressure volume (see Fig. 2), moves up with volume compression and intercepts the Fermi level at this volume, creating a new Fermi surface sheet around point X of the BZ (middle panel), causing an electronic topological transition. This is also reflected in the partial p DOS (bottom panel) of N, whose main peak now cuts the Fermi level. Therefore, the increased hybridization of Th d and f states and N p states at sufficiently high pressure decreases the ionicity, which can alter the balancing attractive and repulsive forces between nearest neighbors significantly, thus destabilizing the NaCl structure and leading to phonon softening. Figure 8 also shows the electronic DOS of ThN in the CsCl structure at the same volume. In this case, the main N p DOS lies 2 eV below E_F, and the main peak for Th f DOS lies 1 eV above E_F. Therefore, in the CsCl structure, even at high pressure, the system maintains its ambient-like bonding, which is also reflected in the band structure and thus in the Fermi surface (middle panel). Comparing total DOS after the phase transition, we found that the CsCl phase has a lower DOS (0.56 states/eV-f.u.) than the NaCl phase (0.99 states/eV-f.u.) at E_F for a given volume (26.99 Å^3 f.u.$^{-1}$); hence, it is favored because of lower one-electron contributions (band energy) to the total energy. It is to be noticed that, for a given volume, the CsCl structure will have larger nearest neighbor distances than that of the NaCl structure. This is consistent with the smaller orbital overlap among neighboring atoms for the CsCl structure. Therefore, when the Th-N bond lengths in the NaCl structure reach some critical value, the increased Coulomb repulsion, arising from the orbital overlap, destabilizes the structure, and the system makes a transition to the CsCl structure to reduce Coulomb repulsion.

To understand why the NaCl structure becomes elastically unstable under pressure only in UN and what the role of f electrons is, we compared the electronic structures at ambient and at high pressures. Figure 9 shows the electronic band

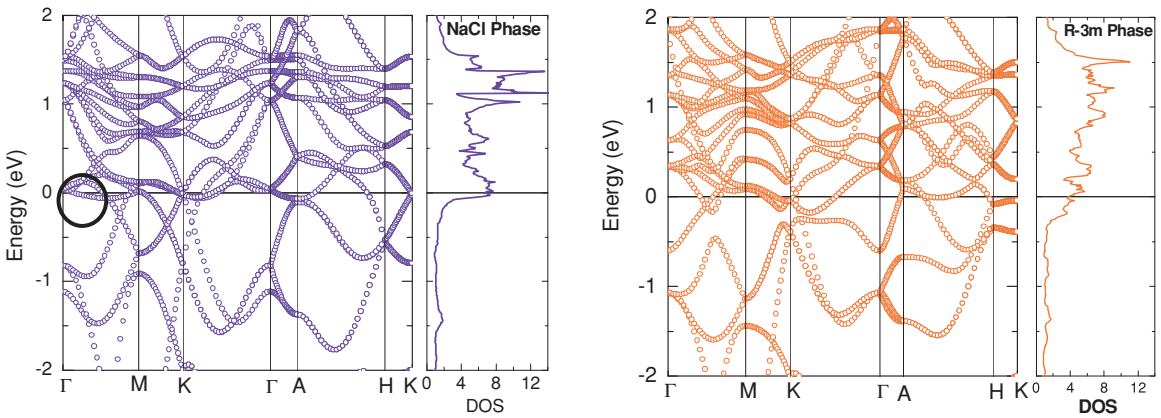

FIG. 9. (Color online) The GGA electronic band structures and electronic density of state (DOS) functions of UN in the NaCl and R-3m phases at a volume of 25.8 Å^3 f.u.$^{-1}$. The band structures are shown along the high-symmetry directions of the hexagonal Brillouin zone for both structures.

structure and DOS functions of UN for NaCl and R-3m at a volume smaller than the transition volume. Compared with ambient pressure, the U *d* and *f* states and N *p* states show slight larger overlap at high pressure (18 GPa) because of band broadening. The *f* band moves to lower energy under pressure. At high pressure, we found the inclusion of on-site Coulomb interactions has a negligible effect because it produces no remarkable change in the DOS functions. The position and band width of the *f* band is crucial because it is known that[39] the systems with a narrow band close to the Fermi level can lower their energy through Peierls-like distortions. In this mechanism, the elastic distortions lower the symmetry of the system, which lifts the degeneracy of one-electron states so that the weight transfers from higher to lower energies in the electronic DOS functions. Thus, the system gains energy by lowering band energy of the electrons, which is used to distort the structure. To see whether the same mechanism is acting in UN, we compared total electronic DOS at E_F for both NaCl and R-3m structures. We found that the R-3m structure has almost half the total DOS at E_F (3.74 states/eV-f.u.) as NaCl (7.39 states/eV-f.u.); hence, the band energy will be lower in this structure. The band structure clearly shows flat *f* bands just above E_F in the NaCl structure (at Γ point indicated by circle), whereas that for R-3m shifted away from E_F because of lower symmetry, consistent with the lower DOS at E_F for the R-3m structure. Hence, we conclusively showed that the underlying mechanism of the NaCl to R-3m phase transition in UN is a Peierls-like distortion that occurred mainly because of the presence of U *f* states just above the Fermi level.

IV. CONCLUSIONS

We have presented the pseudopotential density functional theoretical results of electronic, vibrational, elastic, and structural properties of ThN and UN over the pressure region of 0−100 GPa. Also, we have studied the validity of the LDA and GGA exchange correlations in describing the ground-state and high-pressure properties of these compounds. The LDA is found inadequate, especially for UN; however, the GGA is found to work reasonably well for both compounds. The calculated elastic constants of UN, particularly C_{12} and C_{44}, indicate that even with the GGA second-neighbor, U-U interactions are not accounted for correctly. Detailed electronic structure analysis showed that although both ThN and UN crystallize in the NaCl structure at zero pressure, they have very different electronic behavior that arises because of the *f* electrons present in UN. A phase transition from the NaCl to CsCl structure is found for ThN at 72.5 GPa. Acoustic phonon softening, caused by electronic topological transition, is found to be responsible for this structural transition. In UN, we predict a NaCl to R-3m structural transition near 18 GPa, consistent with earlier experimental observations. Here, the mechanism is completely different; a Peierls-type distortion that occurs because of the *f* bands near the Fermi level is responsible for the elastic instability and structural phase transition. Therefore, the *f* electrons play a crucial role in stabilizing the R-3m structure at high pressure for UN. By taking into account the on-site Coulomb interactions for U 5*f* states, we find that it improves the ambient pressure lattice constant slightly but does not affect the phase transition sequence. However, it changes transition pressure from 18 to 26.5 GPa.

ACKNOWLEDGMENTS

We thank Dr. S. M. Sharma and Dr. L. M. Ramaniah for fruitful discussions.

*ashokverma77@gmail.com

[1] International Nuclear Societies Council (INSC), *A Vision for the Second Fifty Years of Nuclear Energy, Technical Report* (American Nuclear Society, 1996).
[2] J. Adachi, K. Kurosaki, M. Uno, and S. Yamanaka, J. Alloys Compd. **394**, 312 (2005), and references therein.
[3] D. Sedmidubský, R. J. M. Konings, and P. Novák, J. Nucl. Mater. **344**, 40 (2005).
[4] M. S. S. Brooks, J. Magn. Magn. Mater. **29**, 257 (1982).
[5] M. S. S. Brooks, J. Phys. F: Met. Phys. **14**, 857 (1984).
[6] H. L. Skriver, O. K. Anderson, and B. Johansson, Phys. Rev. Lett. **44**, 1230 (1980).
[7] S. K. Chan, J. Phys. Chem. Solids **32**, 1111 (1971).
[8] B. R. Cooper, J. Magn. Magn. Mater. **29**, 230 (1982).
[9] M. S. S. Brooks and P. J. Kelly, Phys. Rev. Lett. **51**, 1708 (1983).
[10] R. Atta-Fynn and A. K. Ray, Phys. Rev. B **76**, 115101 (2007).
[11] N. A. Curry, Proc. Phys. Soc. London **86**, 1193 (1965).
[12] R. Troc, J. Solid State Chem. **13**, 14 (1975).
[13] P. R. Norton, R. L. Tapping, D. K. Creber, and W. J. L. Buyers, Phys. Rev. B **21**, 2572 (1980).
[14] T. M. Holden, W. J. L. Buyers, E. C. Svensson, and G. H. Lander, Phys. Rev. B **30**, 114 (1984).
[15] L. Gerward, J. Staun Olsen, U. Benedict, J.-P. Itie, and J. C. Spirlet, J. Appl. Cryst. **18**, 339 (1985).
[16] J. Staun Olsen, L. Gerward, and U. Benedict, J. Appl. Cryst. **18**, 37 (1985).
[17] J. P. Perdew and Y. Wang, Phys. Rev. B **45**, 13244 (1992).
[18] J. P. Perdew, K. Burke, and M. Ernzerhof, Phys. Rev. Lett. **77**, 3865 (1996).
[19] F. Birch, J. Geophys. Res. **83**, 1258 (1978).
[20] D. Alfè, G. D. Price, and M. J. Gillan, Phys. Rev. B **64**, 045123 (2001).
[21] B. B. Karki, G. J. Ackland, and J. Crain, J. Phys.: Condens. Matter **9**, 8579 (1997).
[22] G. Kresse and J. Hafner, J. Phys.: Condens. Matter **6**, 8245 (1994).
[23] G. Kresse and J. Furthmuller, Comput. Mater. Sci. **6**, 15 (1996).
[24] P. E. Blöchl, Phys. Rev. B **50**, 17953 (1994).
[25] G. Kresse and D. Joubert, Phys. Rev. B **59**, 1758 (1999).
[26] S. L. Dudarev, G. A. Botton, S. Y. Savrasov, C. J. Humphreys, and A. P. Sutton, Phys. Rev. B **57**, 1505 (1998).

[27]Q. Yin, A. Kutepov, K. Haule, G. Kotlair, S. Y. Savrasov, and W. E. Pickett, e-print arXiv:1012.2412 (to be published).
[28]H. J. Monkhorst and J. D. Pack, Phys. Rev. B **13**, 5188 (1976).
[29]D. Alfè (1998). Program available at [http://chianti.geol.ucl.ac.uk/∼dario].
[30]L. Petit, A. Svane, Z. Szotek, W. M. Temmerman, and G. M. Stocks, Phys. Rev. B **80**, 045124 (2009).
[31]M. D. Salleh, J. E. Macdonald, G. A. Saunders, and P. de V. Du Plessis, J. Matter. Sci. **21**, 2577 (1986).
[32]F. A. Wedgwood, J. Phys. C: Solid State Phys. **7**, 3203 (1974).
[33]G. J. Ackland, Rep. Prog. Phys. **64**, 483 (2001), and references therein.
[34]J. A. Jackman, T. M. Holden, W. J. L. Buyers, P. de V. Du Plessis, O. Vogt, and J. Genossar, Phys. Rev. B **33**, 7144 (1986).
[35]A. K. Verma and P. Modak, e-print arXiv:0704.0696 (to be published).
[36]A. K. Verma and P. Modak, Europhys. Lett. **81**, 37003 (2008).
[37]A. Landa, P. Söderlind, A.V. Ruban, O. E. Peil, and L. Vitos, Phys. Rev. Lett. **103**, 235501 (2009).
[38]W. Luo, R. Ahuja, Y. Ding, and H-K. Mao, PNAS **104**, 16428 (2007).
[39]P. Söderlind, O. Eriksson, B. Johansson, J. M. Wills, and A. M. Boring, Nature **374**, 524 (1995).